

ČESKÉ VYSOKÉ UČENÍ TECHNICKÉ V PRAZE
FAKULTA STAVEBNÍ

CZECH TECHNICAL UNIVERSITY IN PRAGUE
FACULTY OF CIVIL ENGINEERING

Ing. Vít Šmilauer, Ph.D.

Mikromechanická analýza silikátových materiálů

Micromechanical Analysis of Silicate Materials

Summary

Micromechanical analysis is becoming a common tool for the analysis of heterogeneous materials. This habilitation lecture summarizes theoretical background and, above all, the application of micromechanics to the group of silicate materials. Portland cement and alkali-activated fly ash are considered as two distinct representatives of a silicate binder.

Chapter 1 introduces silicate materials and their role as a binder. Oxide composition gives an overview of suitable area of Ca-rich and Ca-low compositions.

Chapter 2 shows a multiscale nature of silicate materials and separates them in four scales. Volumetric models for hydrating Portland cement and alkali-activated fly ash are introduced. The spacial and discrete hydration model CEMHYD3D is briefly discussed.

Chapter 3 demonstrates the application of homogenization methods to elasticity and viscoelasticity (creep). Nanoindentation provides intrinsic elastic properties of constituents. Sensitivity analysis for Portland cement gives an impact of input parameters for elasticity. The extension from cement paste to the level of concrete is demonstrated on a few examples; either in one material point or in Gaussian points of FEM. The chapter closes with the micromechanical identification of C-S-H creep properties during basic creep of two-year old cement paste.

Souhrn

Mikromechanická analýza se stává běžnou součástí analýzy heterogenních materiálů. Tato habilitační přednáška shrnuje teoretické pozadí a především aplikaci mikromechaniky na skupinu silikátových materiálů. Portlandský cement a alkalicky aktivovaný popílek jsou uvažovány jako dva rozdílní zástupci silikátových pojiv.

Kapitola 1 uvádí silikátové materiály a jejich roli jako pojiva. Složení z hlediska oxidů ukazuje vhodnou oblast ať už bohatých či chudých na vápník.

Kapitola 2 ukazuje víceúrovňovou povahu silikátových materiálů a rozlišuje čtyři úrovně. Jsou ukázány objemové modely pro hydratující portlandský cement a alkalicky aktivovaný popílek. Dále je krátce pojednáno o prostorovém a diskrétním hydratačním modelu CEMHYD3D.

Kapitola 3 ukazuje aplikaci homogenizačních metod na elasticitu a viskoelasticitu (dotvarování). Nanoindentace poskytuje charakteristické elastické vlastnosti pro jednotlivé chemické složky. Citlivostní analýza pro portlandský cement ukazuje na roli jednotlivých vstupních parametrů pro elasticitu. Rozšíření z cementové pasty na úroveň betonu je ukázáno na několika příkladech: buď na materiálovém či Gaussově bodě v metodě konečných prvků. Kapitola se uzavírá mikromechanickou identifikací parametrů dotvarování C-S-H v saturovaném prostředí vodní páry (basic creep) na vzorku starém dva roky.

Klíčová slova: mikromechanická analýza, charakteristické vlastnosti, nanoindentace, elasticita, homogenizace, metoda Mori-Tanaka, samokonzistentní metoda, dotvarování, dotvarování C-S-H, cementová pasta, N-A-S-H gely.

Keywords: Micromechanical analysis, intrinsic properties, nanoindentation, elasticity, homogenization, Mori-Tanaka method, self-consistent method, basic creep, C-S-H creep, cement paste, N-A-S-H gels.

Contents

1	Silicate construction materials	6
2	Description of microstructure evolution	7
2.1	Volumetric representation	7
2.2	Discrete hydration model CEMHYD3D	8
3	Micromechanical analysis	9
3.1	Elasticity	10
3.1.1	Extension to the level of concrete	13
3.2	Identification of C-S-H creep	15
4	Conclusions	16
	References	17
	Curriculum Vitae	19

1 Silicate construction materials

Silicate materials play a prominent role in the construction sector. A typical representative, concrete, belongs to the most widely produced man-made material due to a low cost, local availability and enhanced durability. On the other hand, over 50 % of all waste in Europe comes from the construction sector. Enormous potential for savings in cost, energy, and resources is foreseeable and necessary in the near future.

Fig. 1 shows that unhydrated Portland cement, patented in 1824 by J. Aspdin, covers only a small area on the diagram. The main hydration product C-S-H is a well-known component with predictable properties. Other binding and secondary materials low in CaO can be utilized as well; slag, fly-ash, or metakaolin. These can be intermixed as a puzzolans with Portland cement or entering alone the process of alkali activation resulting to N-A-S-H gels. [Gluchovskij, 1959] was the first, who systematically studied the alkali activation process. The main reaction product, N-A-S-H gel, is much less understood in terms of its properties. However, the coexistence of C-S-H and N-A-S-H gels was found beneficial for the production of optimal binder composition.

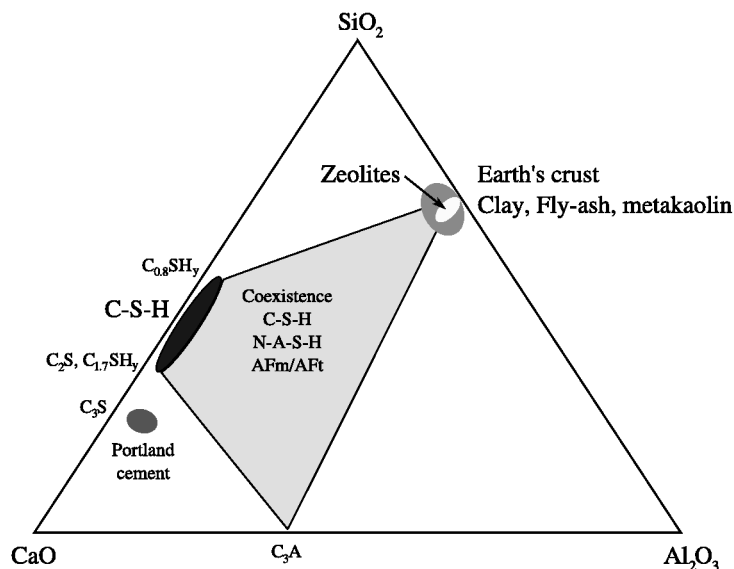


Figure 1: Composition of Portland cement and the area of suitable hydrate phase assemblage.

Introduction of new silicate materials and their optimization lead logically to the question whether durability or life-cycle cost of such new materials can be guaranteed. Experiments do not address true long-term properties hence other predictive methods, such as micromechanics, bring valuable understanding from another perspective.

The aim of this work is the application of micromechanical methods for the assessment of elasticity and viscoelasticity. Silicate materials used in the construction sector and known for their multiscale nature and for the change of properties during maturing stage. Cement paste and alkaline activated fly ash will be considered as the two representatives. Formulated and applied tools fit in the framework of virtual laboratory.

2 Description of microstructure evolution

Concrete manufactured from Portland cement and alkali-activated fly ash belong to a group of multiscale materials. Separation of characteristic length scales significantly simplifies the analysis. Each scale contains dominant chemo-physical phenomena which are identified and analyzed

gel level typically spans the characteristic length between 10 nm – 1 μm ,

- Two morphologies of C-S-H_{LD} and C-S-H_{HD} were found [Bernard et al., 2003],
- N-A-S-H gel in alkali-activated materials with a strong effect of syneresis,

micrometer level is found on the scale between 1 μm and 100 μm ,

- Clinker minerals, gypsum, portlandite, homogenized C-S-H and some capillary porosity are present [Bernard et al., 2003],
- Unreacted fly ash, mullite, vitreous silicates, and slags can be distinguished

mortar level is considered on the scale between 1 mm and 1 cm. The matrix is made from the binder surrounded by fine aggregates. Transition zone appears on the interface in the thickness 0 – 50 μm . Entrained air voids may be found too,

concrete level spans the characteristic length of 1 cm – 1 dm. Mortar, coarse aggregates such as gravel, associated ITZ, and entrapped air are typically identified.

Fig. 2 shows different morphologies at the micrometer level. While C-S-H gel forms in the vicinity of cement grains by a precipitation process, N-A-S-H gel originates from the solution by a polycondensation reaction.

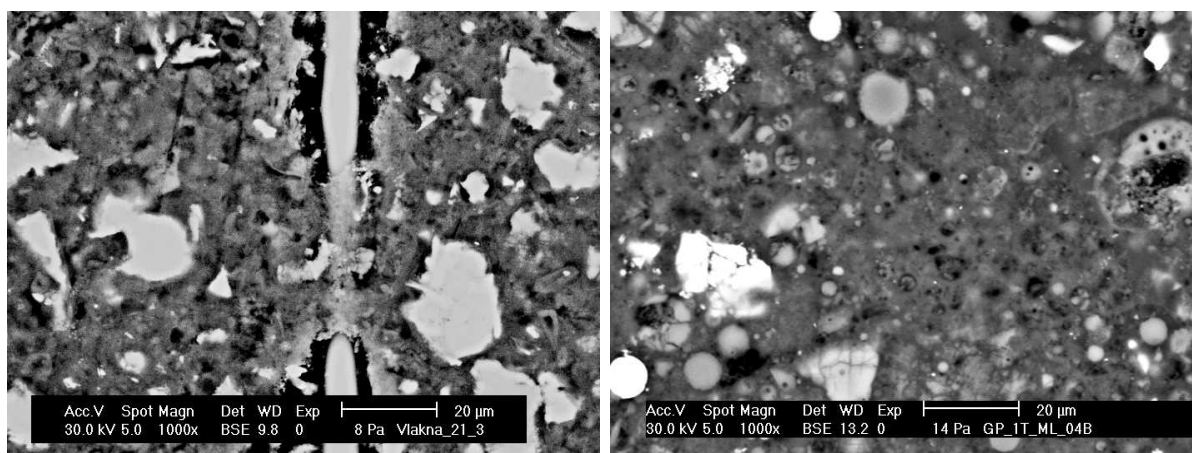


Figure 2: Microstructure of cement paste (left) and alkali-activated fly ash (right). Note a transition zone around a fiber in the cement paste (images by L. Kopecký).

2.1 Volumetric representation

The first coherent and quantitative model for the hydration of cement was deduced by T.C. Powers and his co-workers from data based on water adsorption isotherms [Powers and Brownayards, 1948]. Powers has already distinguished capillary, gel and non-evaporable water. Knowing the degree of hydration (DoH) or indirectly the fraction of non-evaporable water, the volumetric fractions of cement gel, gel water, non-evaporable

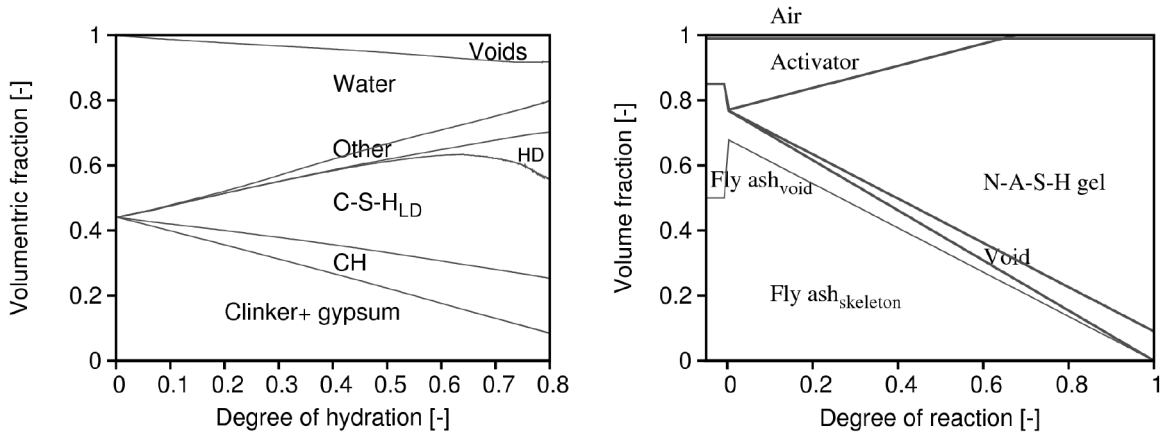


Figure 3: Evolution of volumetric fractions in the system of cement paste (left) and alkali-activated fly ash (right).

water and unhydrated cement may be quantified. Prediction of volumetric phases is depicted in Fig. 3 for the cement paste with $w/c = 0.4$ [Boumiz et al., 1996].

The volumetric model for alkali-activated fly ash was proposed recently [Šmilauer and Němeček, 2007]. The model is based on the assumption of negligible chemical shrinkage and linearity. The N-A-S-H gel in Fig. 3 contains a portion of capillary porosity smaller than approximately $1 \mu\text{m}$. This is due to a coincidence with the resolution of nanoindentation where intrinsic properties will be assigned to N-A-S-H gel intermixed with the porosity.

2.2 Discrete hydration model CEMHYD3D

More detailed analysis of the cement microstructure requires an universal robust model that would capture microstructural evolution within realistic types of cements. The CEMHYD3D hydration model developed at NIST has been adopted and modified [Bentz, 2000, Šmilauer and Bittnar, 2006]. The idea is to split up a microstructure into voxels (volume elements), typically with the size of $1 \times 1 \times 1 \mu\text{m}$.

The 3D microstructure, forming a representative volume element (RVE), consists of chemical phases that are implemented as an ID assignment to each voxel. Cellular automata define the rules how the voxels dissolve, move and what happens on their collision. A flowchart of the model with standard outputs is depicted in Fig. 4.

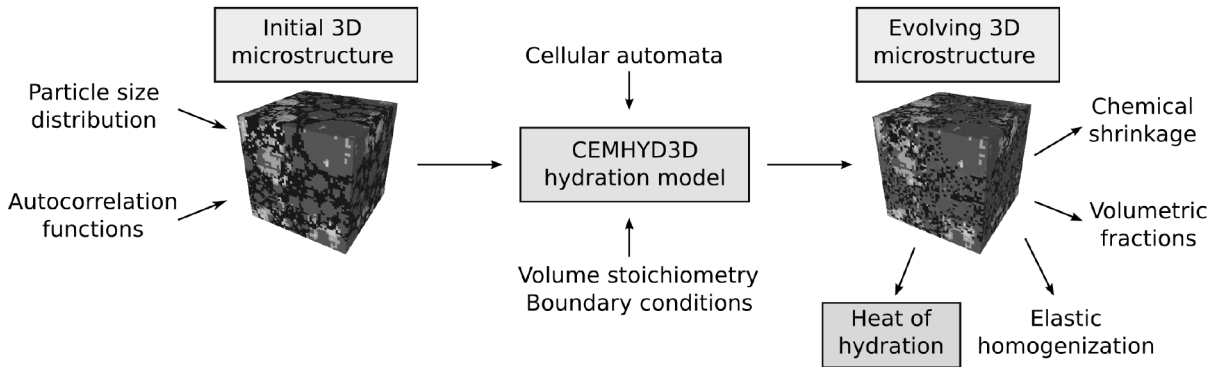


Figure 4: A flowchart of CEMHYD3D model with extensions.

Any model of a random system brings two sources of error: statistical fluctuation and finite size effect [Garboczi and Bentz, 2001]. Statistical error emerges in any random system due to its representation, e.g. small dimensions of a cement paste. Finite size of RVE captures only a limited piece of material which means that the sample may not be statistically representative. This problem may be properly addressed, when the RVE is compared to a sufficiently large RVE.

A loose microstructure would be more susceptible to the RVE size due to lower statistical isotropy. The authors of the CEMHYD3D models suggest minimal size of $100 \times 100 \times 100 \mu\text{m}$ [Garboczi and Bentz, 2001]. Five random realizations were generated for each RVE size and degrees of hydration plotted for $w/c = 0.25$ and 0.5 , Fig. 5. Ordinary Portland cement was used [Kamali et al., 2004]. It becomes clear that $50 \times 50 \times 50 \mu\text{m}$ suffices for a general analysis.

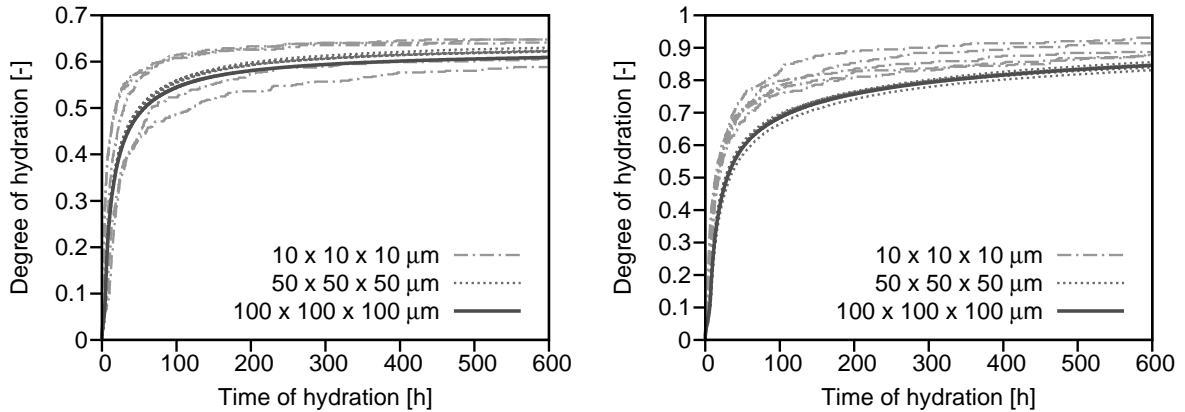


Figure 5: Degree of hydration at five random realizations for each RVE size, $w/c = 0.25$ (left) and $w/c = 0.5$ (right).

3 Micromechanical analysis

Micromechanical analysis allows to predict properties from a lower scale (upscaling) or to identify properties of a certain constituent from a higher scale (downscaling). A series of homogenization steps may bridge several levels and this approach will be exemplified to arrive at elastic properties of concrete. Several methods used in this work can accomplish the micromechanical analysis

analytical methods require typically volume fractions and intrinsic properties of constituents

- Mori-Tanaka scheme assumes a matrix filled with inclusions [Mori and Tanaka, 1973],
- self-consistent scheme assumes that matrix and inclusions are indistinguishable [Hill, 1965],

numerical methods requiring, in addition, knowledge of spatial distribution of phases and specifying the type of boundary condition

- Finite element method (FEM) solving static equilibrium equations [Šmilauer and Bittnar, 2006],

- Fast Fourier transform (FFT)-based method allowing only periodic boundary conditions [Moulinec and Suquet, 1994].

3.1 Elasticity

In the case of elasticity, intrinsic elastic properties of phases must be acquired, typically by a nanoindentation technique, Tab. 1. Complete list of phases is available [Bernard et al., 2003, Šmilauer and Bittnar, 2006].

Phase	Young's modulus [GPa]	Poisson's ratio [-]
C ₃ S	135±7	0.3
C ₂ S	130±20	0.3
C ₃ A	145±10	0.3
C ₄ AF	125±25	0.3
CH	38±5	0.305
C-S-H _{LD}	21.7±2.2	0.24
C-S-H _{HD}	29.4±2.4	0.24
Fly ash	84.7± 6.6	0.2
N-A-S-H gel	30.9± 4.7	0.25
Water ^a	10 ⁻³	0.499924
Empty pore	10 ⁻³	10 ⁻³

Table 1: Intrinsic elastic properties of dominant chemical phases as measured by nanoindentation. Results for cement paste and alkali-activated fly ash.

^a water bulk modulus 2.19 GPa

Fig. 6 gives the results of analytical and numerical homogenization technique for silicate materials. Two-level analytical homogenization procedure starts at the level of C-S-H and the upscaled results are transferred to the level of cement paste. Volume fractions correspond to Fig. 3 with $w/c = 0.4$ [Boumiz et al., 1996]. Mori-Tanaka and the self-consistent scheme are employed. In addition, the results from FFT-based homogenization on $75 \times 75 \times 75 \mu\text{m}$ are shown for a comparison. Homogenization of alkali-activated fly ash follows only analytical methods due to the lack of spatial distribution of phases.

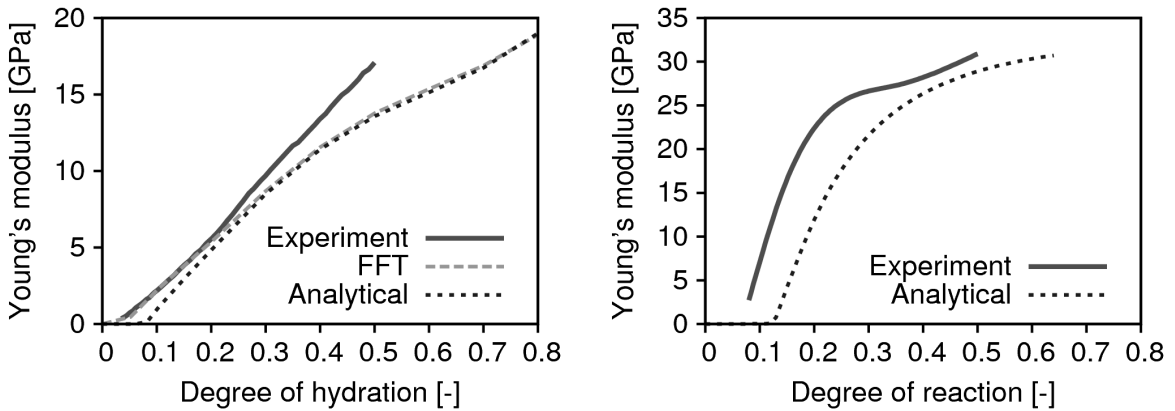


Figure 6: Homogenization of cement paste (left) and alkali-activated fly ash (right) by a two-level analytical or FFT-based homogenization method.

The type of boundary conditions controls the overall response resulting in different effective elastic properties. Fig. 7 demonstrates the effect of capillary porosity on the Young modulus. Cement paste with $w/c = 0.25$ is hydrated to 30 % (porosity fraction 0.25) and than to 62 % (porosity fraction 0.05). High porosity fraction in the less hydrated cement leads to a large scatter with regards to imposed boundary conditions [Kanit et al., 2003]. Periodic boundary conditions yield the most stable effective values when the microstructure size changes.

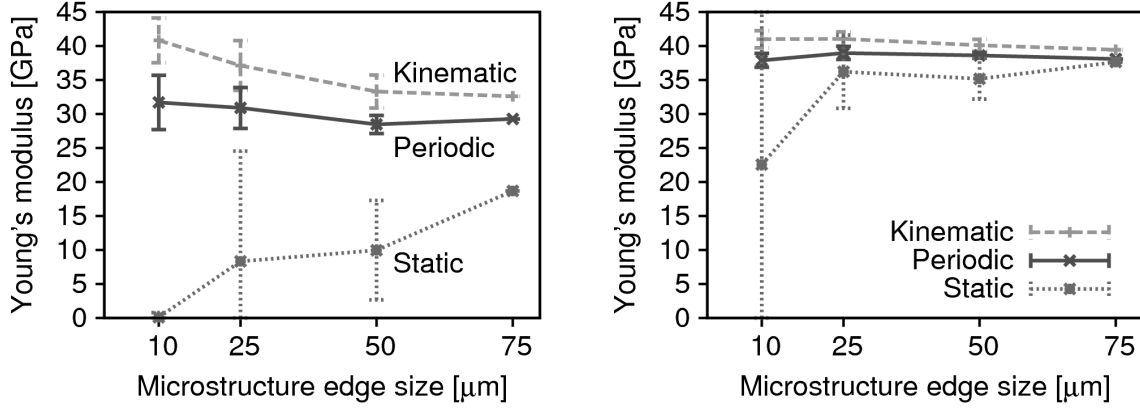


Figure 7: Effect of static, kinematic and periodic boundary conditions. Cement paste $w/c = 0.25$ hydrated to 30 % (left) and 62 % (right).

Combination of the hydration model and elastic homogenization allows to explore sensitivity of input parameters for the effective elastic properties. Tab. 2 summarizes the ranges of input parameters. The values were selected based on [Taylor, 1990] which are typical for Portland cements used today worldwide.

Parameter	Units	Minimum	Maximum
Blaine fineness	[m ² /kg]	200	600
Gypsum content	[cement vol. fraction]	0	0.1
Autocorrelation file num.	-	0	9
C ₃ S	[cement mass fraction]	0.4	0.8
C ₂ S	[cement mass fraction]	0	0.35
C ₃ A	[cement mass fraction]	0	0.15
C ₄ AF	[cement mass fraction]	0	0.15
W/c	-	0.2	0.6
Curing condition regime	-	0-saturated	1-sealed

Table 2: Range of input parameters used in the sensitivity analysis

Determination of Young's modulus is based on linear elastic homogenization, utilizing FFT method on percolated periodic microstructures [Šmilauer and Bittnar, 2007]. The computational volume from CEMHYD3D is sampled to a grid of 50 x 50 x 50 Fourier points. The numerical FFT homogenization is an iterative procedure

$$\boldsymbol{\varepsilon}^{k+1}(\mathbf{x}) = \boldsymbol{\varepsilon}^k(\mathbf{x}) - \int_V \boldsymbol{\Gamma}^0(\mathbf{x} - \mathbf{x}') \boldsymbol{\sigma}^k(\mathbf{x}') d\mathbf{x}', \quad (1)$$

where k is an iteration cycle, Γ^0 represents the translation invariant Green operator associated with arbitrary chosen reference medium [Moulinec and Suquet, 1994]. The average time consumption for one FFT-based homogenization is around 10 minutes on 3.2 GHz CPU with $50 \times 50 \times 50$ Fourier points.

Fig. 8 shows the stochastic statistical sensitivity between input parameters and homogenized Young's modulus determined from 200 random realizations. W/c ratio is the only governing parameter, followed by cement fineness. Obviously, lower w/c means lower capillary porosity at the same degree of hydration. The role of fineness can be explained by more uniform distribution of stiff cement grains and hydration products; more homogeneous composites with the same volume fractions are known to exhibit higher stiffness.

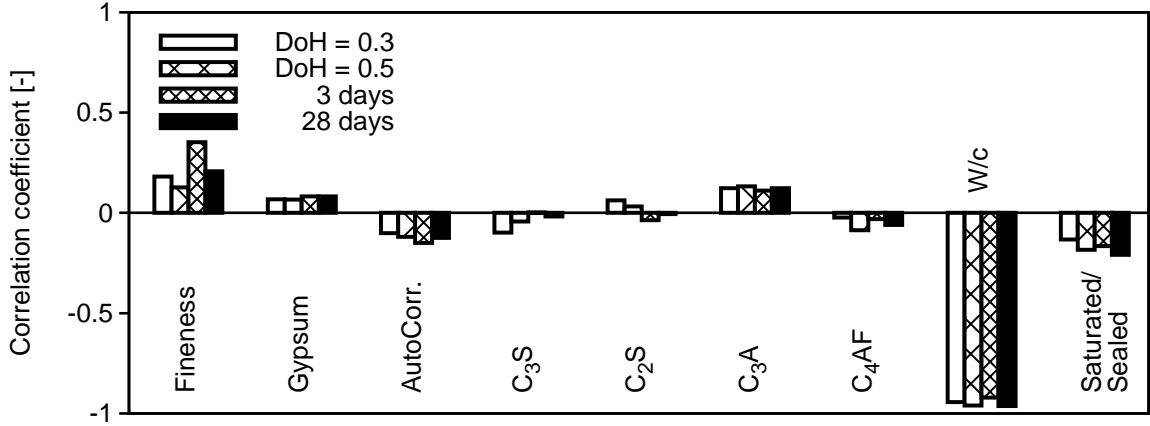


Figure 8: Correlation between input parameters and Young's modulus at two degrees of hydration and two hydration times.

The data from sensitivity analysis can be approximated with analytical power function. The function should match the asymptotes and take into account limit values, such as a percolation threshold at a low hydration degree. The solid percolation threshold was found previously to be the function of w/c [Šmilauer and Bittnar, 2007]. The evolution of Young's modulus against degree of hydration should be concave in all cases. The following equations, valid in the range $0.2 \leq w/c \leq 0.6$, were obtained by nonlinear fitting to equally-weighted points

$$\text{Young's modulus [GPa]} = a(\text{DoH} - \text{DoH}_p)^b \geq 0, \quad (2)$$

$$\text{DoH}_p = 0.0485 w/c, \quad (3)$$

$$a = \frac{1}{0.14 w/c^{1.35}}, \quad (4)$$

$$b = 2.15 w/c - 0.08, \quad b \leq 1. \quad (5)$$

The coefficient a expresses the asymptotic Young's modulus at complete hydration (in fact total hydration does not occur below $w/c = 0.36$ [Hansen, 1986]). For example, the limits follow $a = 62.4$ GPa at $w/c = 0.2$ and $a = 13.56$ GPa at $w/c = 0.6$. The coefficient b quantifies the concavity which is known to be higher in lower w/c , i.e. the Young's modulus progresses faster in a lower DoH regardless on a . Coefficient b is limited by 1.

The maximum Young's modulus from all considered Portland cement pastes can attain approximately 50 GPa for $w/c = 0.2$. For this particular case, the maximum degree of hydration is 0.55. The stiffness in low w/c is high due to large amounts of unhydrated clinker minerals, with greater contribution than the amount of formed C-S-H filling up the capillary porosity. The correlation coefficient between Eq. (2) and the data yields 0.986 and the plot for different degrees of hydration is displayed in Fig. 9.

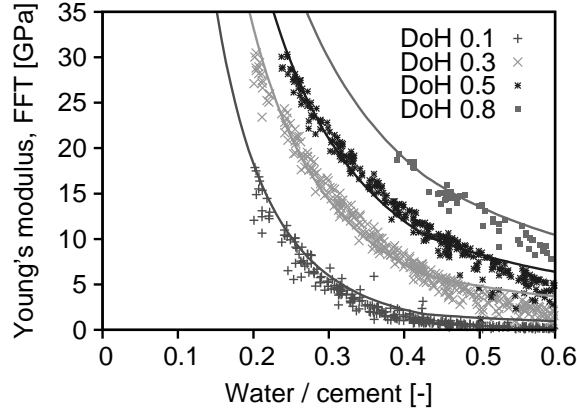


Figure 9: Simulation and the approximation of effective Young's modulus by Eqs. (2)-(5).

3.1.1 Extension to the level of concrete

The transition of homogenized elastic properties among levels and applied homogenization schemes are described in Fig. 10. Elastic homogenization is based solely on analytical approach. Adopted methodology is very efficient in terms of time consumption and reasonable accuracy of results [Šmilauer, 2006].

The level of cement paste captures the effect of secondary cementitious material (SCM), inert filler and entrained air. All mentioned phases are present in minor amount, therefore Mori-Tanaka scheme considers reference phase as the virgin cement paste.

Mortar level is homogenized via Hervé-Zaoui scheme [Hervé and Zaoui, 1993], where fine aggregate represents the most inner spherical inclusion. It is surrounded with the fraction of ITZ with reduced Young's modulus to the half of that from cement paste level. Poisson's ratio remains unchanged. The third concentric shell is represented by the cement paste and all these three phases are embedded in an unknown medium whose properties are determined. Homogenization of concrete follows the same approach as in the mortar level. The results for concrete [Lee et al., 2004] with $w/c = 0.27$ and 0.5 are displayed in Fig. 11 and are in reasonable agreement with experiment.

Fig. 12 shows further extension of homogenization from a material point to Gaussian points on a 2D cross section. The figure displays casting of a beam on an old slab on a new railway scaffold bridge in Prague. The maximum beam width was 1.65 m and height 2.15 m. Eight $50 \times 50 \times 50 \mu\text{m}$ microstructures of cement paste formed the basis of elastic homogenization. Whole beam simulation took 68 minutes on 3.2 GHz PC and occupied 19 MB of RAM. Calculations covered 10 days of hydration.

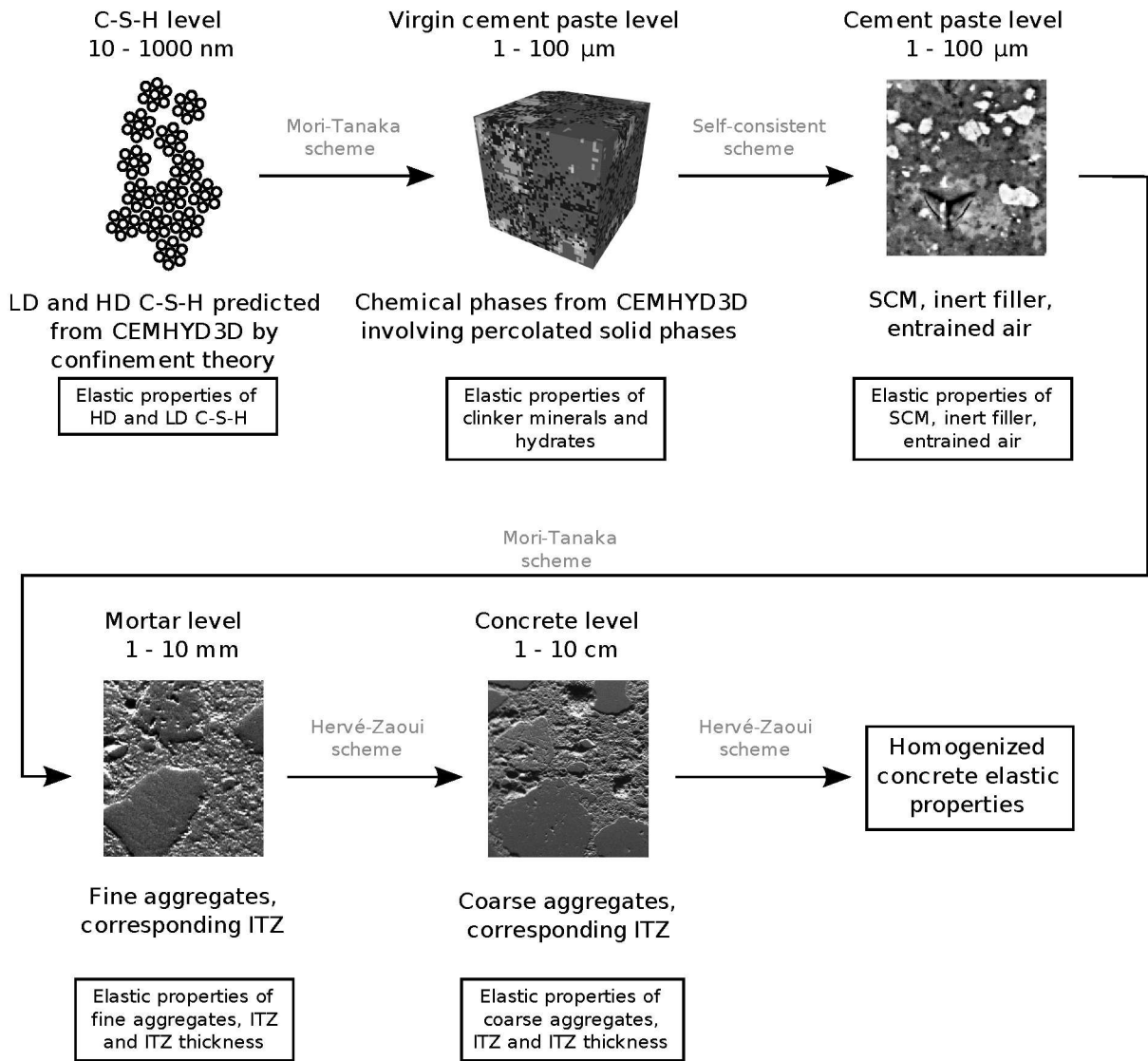


Figure 10: Adopted multiscale elastic homogenization approach.

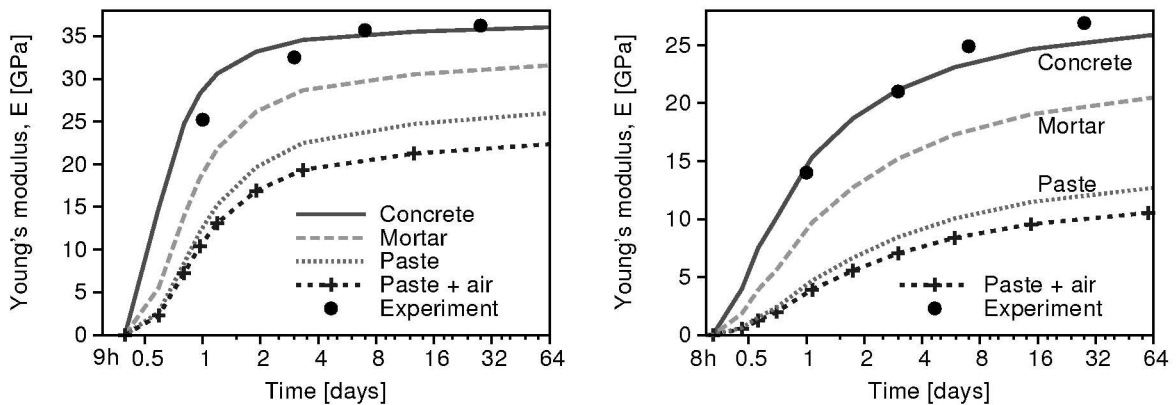


Figure 11: Young's modulus of cement paste, mortar and concrete as predicted from multiscale homogenization, $w/c = 0.27$ (left) and 0.5 (right).

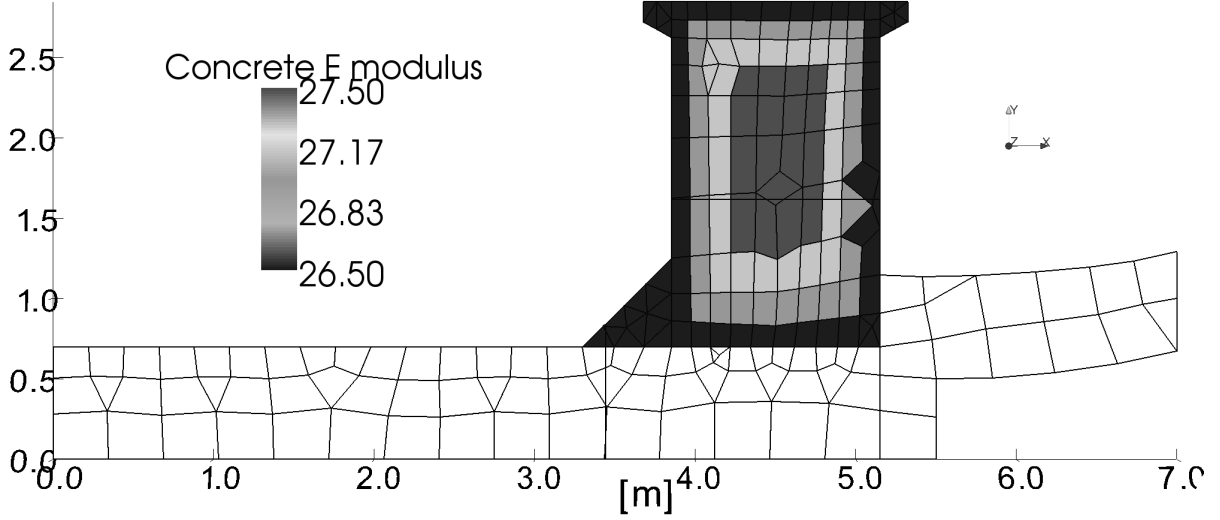


Figure 12: Young's modulus of concrete at 46 hours after casting.

3.2 Identification of C-S-H creep

It has been recognized that creep of cement paste is attributed dominantly to C-S-H phase. Unfortunately, C-S-H can not be prepared synthetically on the macroscopic scale hence the viscous properties must be obtained either on the submicron scale or by means of inverse analysis. Although nanoindentation testified a short-term C-S-H creep, the holding period can not last longer than a few minutes due to device stability. Therefore, the long-term quantification of C-S-H creep has to rely solely on the inverse analysis.

If creep is assigned dominantly to C-S-H phase, the constitutive law must have the same structure as for concrete or cement paste. Constitutive law of B3 model allows to capture aging and irreversible creep in the form [Bažant and Baweja, 2000]

$$J(t, t') = q_1 + C_v(t, t') + q_4 \ln \left(\frac{t}{t'} \right) \quad (6)$$

$$C_v(t, t') = \int_{t'}^t v^{-1}(t) \dot{C}_g(\tau - t') d\tau = \int_{t'}^t v^{-1}(t) \frac{n(\tau - t')^{n-1}}{\lambda_0^n + (\tau - t')^n} d\tau \quad (7)$$

$$v^{-1}(t) = \left[q_2 \left(\frac{\lambda_0}{t} \right)^m + q_3 \right] \quad (8)$$

To simplify the analysis and the identification of unknown parameters, only basic creep is taken into account. FFT-based homogenization method is extended for viscosity using continuous retardation spectrum and exponential algorithm [Jirásek and Bažant, 2002].

The first question coming to the mind is the reversibility of creep. Let us reconstruct an experiment of two-year old cement paste with $w/c = 0.5$ [Beaudoin and Tamtsia, 2004]. The specimens were simultaneously in the process of drying to the RH of 96 %. Parameters $q_1, q_3, q_4, \lambda_0, n$ have to be identified for the C-S-H creeping phase in Eqs. (6)-(8).

Parameter q_4 quantifies the irrecoverable flow strain which can be determined from unloading, independently of the other parameters of mature paste. Parameters q_1 and q_3 are in fact related through nano-indentation data, but are subjected to a certain range of uncertainty, limited by the creep attained.

Two RVEs $10 \times 10 \times 10$ and $50 \times 50 \times 50 \mu\text{m}$ of cement paste were generated using CEMHYD3D model. The fitting to experimental data yields $q_1 = 0.0381 \text{ 1/GPa}$, $q_3 = 0.040 \text{ 1/GPa}$, $q_4 = 0.002 \text{ 1/GPa}$, $\lambda_0 = 1 \text{ day}$, and $n = 0.25$. Fig. 13 shows assigned viscoelastic behavior to C-S-H, in addition without flow term ($q_4 = 0$) to illustrate the effect of irrecoverable creep part. An arrow points to the time when indentation modulus is typically evaluated. The RVE size $50 \times 50 \times 50 \mu\text{m}$ is obviously sufficient and the response does not differ from $10 \times 10 \times 10 \mu\text{m}$, Fig. 13. The concurrence is attributed to a weak heterogeneity due to well hydrated cement paste with the absence of large unhydrated cement grains.

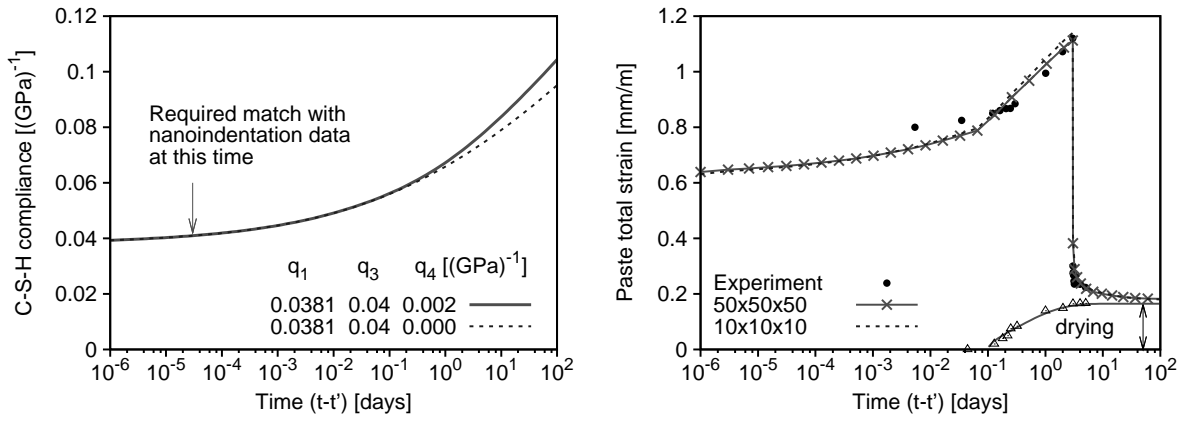


Figure 13: Compliance assigned to C-S-H (left), for comparison without the flow term ($q_4 = 0$). Measured total strain of two-year old cement paste (right) with simulated strain for two microstructure sizes.

4 Conclusions

Micromechanics brings significant benefits for the prediction of elastic properties in multiscale silicate materials such as concrete. Validation shows reasonable agreement at the level of cement paste and concrete. Virtual laboratory quantified statistical sensitivity for Young's modulus and w/c was found to be the only governing parameter.

For the first time, micromechanical inverse analysis quantified parameters of a constitutive law for C-S-H. The simulation reveals that C-S-H must exhibit a slower decay of creep rate with time than does the cement paste or concrete.

Acknowledgement

The formulation and validation of multiscale model were supported by the Ministry of Education, Youth and Sports under the project MSM 6840770003 - Algorithms for computer simulation and application in engineering. Fruitful discussions with professors and colleagues, in particular Z. Bittnar, J. Zeman, T. Krejčí, J. Kruis, T. Koudelka,

M. Jirásek, M. Lepš, Z. Vittingerová, and P. Kabele are greatly appreciated. D.P. Bentz and E.J. Garboczi are acknowledged for the NIST cement hydration model.

References

- [Bažant and Baweja, 2000] Bažant, Z. and Baweja, S. (2000). Creep and shrinkage prediction model for analysis and design of concrete structures: Model B3. Technical report, Am. Concrete Institute.
- [Beaudoin and Tamtsia, 2004] Beaudoin, J. and Tamtsia, B. (2004). Creep of hardened Cement Paste - The role of Interfacial Phenomena. *Interface Science*, 12:353–360.
- [Bentz, 2000] Bentz, D. (2000). CEMHYD3D: A Three-Dimensional Cement Hydration and Microstructure Development Modeling Package. Version 2.0. Technical report, NIST Building and Fire Research Laboratory, Gaithersburg, Maryland.
- [Bernard et al., 2003] Bernard, O., Ulm, F.-J., and Lemarchand, E. (2003). A multiscale micromechanics-hydration model for the early-age elastic properties of cement-based materials. *Cem. Concr. Res.*, 33(9):1293–1309.
- [Boumiz et al., 1996] Boumiz, A., Vernet, C., and Tenoudji, F. (1996). Mechanical Properties of Cement Pastes and Mortars at Early Ages. *Advanced Cement Based Materials*, 3(3-4):94–106.
- [Garboczi and Bentz, 2001] Garboczi, E. and Bentz, D. (2001). The effect of statistical fluctuation, finite size error, and digital resolution on the phase percolation and transport properties of the NIST cement hydration model. *Cem. Concr. Res.*, 31(10):1501–1514.
- [Gluchovskij, 1959] Gluchovskij, V. (1959). *Gruntosilikaty*. Gosstrojizdat USSR, Kiev.
- [Hansen, 1986] Hansen, T. (1986). Physical structure of hardened cement paste. A classical approach. *Matériaux et Constructions*, 114(19):423–436.
- [Hervé and Zaoui, 1993] Hervé, E. and Zaoui, A. (1993). N-layered Inclusion-based Micromechanical Modelling. *Int. J. Engng Sci.*, 31:1–10.
- [Hill, 1965] Hill, R. (1965). Theory of mechanical properties of fiber-strengthened materials. - III: Self-consistent model. *J. Mech. Phys. Solids*, 13:189–198.
- [Jirásek and Bažant, 2002] Jirásek, M. and Bažant, Z. (2002). *Inelastic analysis of structures*. John Wiley & Sons, Ltd.
- [Kamali et al., 2004] Kamali, S., Moranville, M., Garboczi, E., Prené, S., and Gérard, B. (2004). Hydrate dissolution influence on the young’s modulus of cement paste. In et al., L., editor, *Proc. Fracture Mechanics of Concrete Structures (FraMCoS-V)*, pages 631 – 638, Vail.
- [Kanit et al., 2003] Kanit, T., Forest, S., Galliet, I., Mounoury, V., and Jeulin, D. (2003). Determination of the size of the representative volume element for random composites: Statistical and numerical approach. *International Journal of Solids and Structures*, 40:3647–3679.

- [Lee et al., 2004] Lee, H., Lee, K., Kim, Y., Yim, H., and Dae, D. (2004). Ultrasonic in-situ monitoring of setting process of high-performance concrete. *Cem. Concr. Res.*, 34:631–640.
- [Mori and Tanaka, 1973] Mori, T. and Tanaka, K. (1973). Average stress in matrix and average elastic energy of materials with misfitting inclusions. *Acta Metallurgica*, 21(5):1605–1609.
- [Moulinec and Suquet, 1994] Moulinec, H. and Suquet, P. (1994). A fast numerical method for computing the linear and nonlinear mechanical properties of composites. *Comptes Rendus de l'Academie des Sciences Serie II*, 318(11):1417–1423.
- [Šmilauer, 2006] Šmilauer, V. (2006). *Elastic properties of hydrating cement paste determined from hydration models*. PhD thesis, ČVUT in Prague, Faculty of Civil Engineering.
- [Powers and Brownnyards, 1948] Powers, T. and Brownnyards, T. (1948). Studies of physical properties of hardened portland cement paste. Bulletin 22, Research Laboratories of the Portland Cement Association, Chicago.
- [Taylor, 1990] Taylor, H. (1990). *Cement Chemistry*. Academic Press, New York.
- [Šmilauer and Bittnar, 2006] Šmilauer, V. and Bittnar, Z. (2006). Microstructure-based micromechanical prediction of elastic properties in hydrating cement paste. *Cem. Concr. Res.*, 36(9):1708–1718.
- [Šmilauer and Bittnar, 2007] Šmilauer, V. and Bittnar, Z. (2007). Modelling of Microstructural Evolution of Concrete under Work Conditions and in Hardening Process. In Topping, B., editor, *Civil Engineering Computations: Tools and Techniques*, pages 347 – 367.
- [Šmilauer and Němeček, 2007] Šmilauer, V. and Němeček, J. (2007). Elastic properties of alkaline activated fly ash: results from nanoindentation and micromechanical modeling. In *Alkali Activated Materials - Research, Production and Utilization*, pages 677–688.

Curriculum Vitae

OSOBNÍ ÚDAJE	Ing. Vít Šmilauer, Ph.D. narozen 10.7.1978
VZDĚLÁNÍ	ČVUT v Praze, Fakulta stavební, obor Konstrukce a dopravní stavby, obhajoba disertační práce 2006 (Ph.D.) ČVUT v Praze, Fakulta stavební, obor Konstrukce a dopravní stavby, 1997-2003 (Ing.) TU Delft, Nizozemí, Civil Engineering and Geosciences, 2001 McCrary High School, McCrary, Arkansas, USA, 1996-1997
ZAMĚSTNÁNÍ	2003-2009 ČVUT v Praze, Fakulta stavební, vědecký pracovník, odborný asistent 2000-2003 Di5 s.r.o., architektonicko-projekční kancelář, statika budov
PEDAGOGICKÁ PRAXE	Přednášky z předmětů: Metoda konečných prvků (10+20), Stavební mechanika (10) Cvičení z předmětů: Pružnost, pevnost (10+20), Metoda konečných prvků (10+20), Stavební mechanika (1+10+20), Dynamika stavebních konstrukcí (10), Přetváření materiálů (10) Spolupodílel se na zavedení předmětu Mikromechanika a popis mikrostruktury materiálů, garant Ing. J. Němeček, Ph.D. Vytvoření veřejně přístupných elektronických přednášek z předmětu Stavební mechanika 1 (GNU Free Documentation License)
VĚDECKOVÝZKUMNÁ ČINNOST	Numerické metody mechaniky, homogenizační metody, víceúrovňové modelování Spoluřešitel výzkumného záměru MSM6840770003 (2005-2011). Spolupracovník pěti grantů GAČR, jednoho grantu MŠMT s NSF (USA). Řešená problematika cementových a alkalicky aktivovaných materiálů, jejich dotvarování, počítačové simulace mikrostruktur, dynamické interakce mostu a vozidla.
PUBLIKACE	Za posledních pět let autor monografie, osmi odborných článků v časopisech, přes 20 příspěvků na českých i zahraničních konferencích.